LOS ALAMOS SCIENTIFIC LABORATORY
of the
University of California
LOS ALAMOS • NEW MEXICO

Neutron Cross Sections for ^{239}Pu and ^{240}Pu in the Energy Range 1 keV to 14 MeV

UNITED STATES
ATOMIC ENERGY COMMISSION
CONTRACT W-7405-ENG. 36

This report expresses the opinions of the author or authors and does not necessarily reflect the opinions or views of the Los Alamos Scientific Laboratory.

Printed in the United States of America. Available from
Clearinghouse for Federal Scientific and Technical Information
National Bureau of Standards, U. S. Department of Commerce
Springfield, Virginia 22151
Price: Printed Copy $3.00; Microfiche $0.65

LA-3528
UC-34, PHYSICS
TID-4500

LOS ALAMOS SCIENTIFIC LABORATORY
of the
University of California
LOS ALAMOS • NEW MEXICO

Report written: July 1968
Report distributed: September 4, 1968

Neutron Cross Sections for ^{239}Pu and ^{240}Pu in the Energy Range 1 keV to 14 MeV

by

R. E. Hunter*
J.-J. H. Berlijn**
C. C. Cremer

*Work begun while a LASL Staff Member, completed while in capacity of Consultant. Present address: Physics Department, Valdosta State College, Valdosta, Georgia.

**Present address: Physics Department, Valdosta State College, Valdosta, Georgia.

NEUTRON CROSS SECTIONS FOR ^{239}PU AND ^{240}PU IN THE ENERGY RANGE 1 keV TO 14 MeV

by

R. E. Hunter, J.-J. H. Berlijn, C. C. Cremer

ABSTRACT

Recommended cross sections for ^{239}Pu and ^{240}Pu are presented. Comparisons of calculated and experimental values of integral systems were used as a guide in choosing the fits to microscopic cross-section data.

I. INTRODUCTION

This report presents the results of a compilation of the available experimental data on the neutron-induced reaction cross sections for plutonium isotopes, with the objective of providing consistent sets of cross sections for neutronics calculations in fast critical and super-critical systems. Because of the neutron flux spectra in these very fast systems, cross sections at incident neutron energies of 1 keV and lower are relatively unimportant. Cross sections are presented from 1 keV to 14 MeV.

Extensive comparisons were made with a host of integral experiments, such as bare and reflected critical assemblies, spectral indices, and central core reactivity contribution. Each of these comparisons provided a further check on the experimental data, and in some cases led to alteration of the previously chosen best fit to the data.

Several compilations of experimental and theoretical neutron cross sections already exist in which the author has recommended "best fits" to the data presented. The experimental uncertainty of these data is usually about 5% or greater, and variations in these fits may justifiably be made within this uncertainty. However many integral experiments exist in which certain choices of these fits to the data lead to calculations of the integral quantity which lie outside the range of experimental error.

A good example is the critical mass of plutonium (94.134% ^{239}Pu) which was measured in the Jezebel assembly. The critical mass is known to within ± 0.1%. However, an uncertainty of ± 5% in the fission cross section of ^{239}Pu leads to a calculational uncertainty of ± 13% in the critical mass. It is believed that the calculational techniques available on modern computers are capable of calculating the critical mass of this assembly to ± 0.2%. Integral experiments such as this may therefore be thought of as placing one more constraint upon the "best fit" to the microscopic cross-section data.

The purpose of this report is to present such a set of recommended data which has been found to give agreement within experimental error for all such integral

quantities that have been calculated. It is not intended that these curves should be considered as being a refinement on the experimental data, or "better" in some nebulous sense than the experimental data, nor do the authors contend that the experimental uncertainty in the data has been somehow reduced. All that is claimed is that these recommended curves represent a particular set of fits to the experimental data which is consistent with the integral experiments.

It is recognized, of course, that this recommended set of curves is not unique. However, it is felt that it represents a useful step in the processing of neutron cross-section data for use in neutronics calculations. Indeed, the cross section user may often find that to achieve the degree of accuracy that is required of his calculations a normalization of this type is essential. Needless to say, the final element of responsibility for checking his calculations against those experiments which bear most directly on the problem under study must still fall on the user.

In this respect it should be noted that the sensitivity of the calculations of integral experiments to variations in the cross sections within an energy range is proportional to the total neutron flux within that energy range. Since all integral experiments used in the above tests were performed on fast assemblies, confidence in the recommended curves is highest in the range 0.1 - 6 MeV, and drops at both the low and high ends of the energy range.

This report is not intended to represent a comprehensive compilation of experimental data, with best fits to these data alone. Rather, the best fits were used as initial input to calculations for comparison with the series of integral experiments as described above. These results were then used to modify the initial best fits in such a way that consistent results were obtained for all calculations. Attempts were made to keep these modifications within the experimental errors on the data. In fact, for the cross sections presented in this report, these modifications were 3% or less.

The calculational techniques used in computing the integral experiments were carried to the point at which numerical and calculational approximations introduce errors which are comparable to, or less than, the experimental errors on the integral quantities. These calculations and comparison with the integral experimental results are described in detail in the authors' report LA-3529.[1]

II. CALCULATIONAL PROCEDURE

The energy region of interest extends from 1 keV to 14 MeV. Over this region the cross sections of importance are:

total cross section - $\sigma_{n,T}$
fission cross section - $\sigma_{n,F}$
elastic scattering cross section - $\sigma_{n,n}$
inelastic scattering cross section - $\sigma_{n,n'}$
radiative capture cross section - $\sigma_{n,\gamma}$
(n,2n) cross section - $\sigma_{n,2n}$
(n,3n) cross section - $\sigma_{n,3n}$

To accurately represent the final-state neutron spectra, it is desirable to represent the fission cross section as the sum of three cross sections:

$$\sigma_{n,F} = \sigma_{n,f} + \sigma_{n,n'f} + \sigma_{n,2nf}. \qquad (1)$$

$\sigma_{n,f}$ will denote the direct fission cross section, with $\sigma_{n,F}$ the total fission cross section.

The cross-section data, along with neutron energy and angular distributions, were processed by a digital computer program which calculated a flux-weighted average of each cross section over a specified set of energy groups. These group cross sections were then used in a calculation employing the Carlson discrete S_n approximation to the Boltzmann transport equation to test the cross sections with integral

experiments. The microscopic data were then adjusted where necessary to give agreement with the integral experiments. For details of the calculational techniques the reader is referred to LA-3529.

III. PLUTONIUM-239

For the well-established cross sections, no attempt has been made to catalog every report on the subject; rather a reference is given to an already existing compilation. Individual reports are referenced if they are not included in such a compilation.

A. Total Cross Section

The total cross section is well described by the compilations of Schmidt[2] and Hughes and Schwartz.[3] Between 1 and 10 keV, there is considerable spread in the data, resulting in a rather large uncertainty ($\sim$ 10%) in the total cross section in that energy range.

B. Fission Cross Section

Considerable data exist for the fission cross section. In addition to the compilations of Schmidt and of Hughes and Schwartz, the data of Ferguson and Pattenden,[4] James,[5] and White et al.[6] were used. Although the data of White et al. lie somewhat below those of other authors, they are the most accurate available. Also, these data give much better agreement with integral experiments. Hence, the recommended curve is based largely on these points between 40 and 500 keV.

The thresholds for $\sigma_{n,n'f}$ and $\sigma_{n,2nf}$ are at about 5.5 MeV and 10.5 MeV, respectively. The curves of $\sigma_{n,n'f}$ and $\sigma_{n,2nf}$ are given along with $\sigma_{n,F}$ in Fig. 3.

C. Radiative Capture Cross Section

The radiative capture cross section is based on the compilations of Schmidt,[2] Hughes and Schwartz,[3] Stehn et al.,[7] and Douglas and Barry,[8] and on the data presented by Okrent and Thalgott[9] on the capture-to-fission ratio, α.

D. Elastic Scattering Cross Section

Very few direct measurements of $\sigma_{n,n}$ have been made. However, below about 10 keV we can write

$$\sigma_{n,n} = \sigma_{n,T} - \sigma_{n,\gamma} - \sigma_{n,F}. \qquad (2)$$

From Eq. 2 and the recommended curve of Schmidt,[2] the elastic scattering cross section was established up to 10 keV.

Above 10 keV, this procedure is complicated by the onset of inelastic scattering. There are some data on the scattering cross sections, primarily those of Andreev[10] at 0.9 MeV, Cranberg[11] at 0.55, 0.98, and 2.0 MeV, and Allen[12] from 0.15 to 1.0 MeV. These measurements consist of partial cross sections for ranges of the Q value at a given incident neutron energy, E_n. Since different Q values were used at the same E_n, it was possible in some cases to use subtraction techniques to separate the different cross sections. (See Sect. III-E.)

Also, there are measurements between 8 and 14 MeV of the nonelastic cross section, $\sigma_{n,X}$, given by Stehn et al.[7] and by Degtyarev.[13] From the relation

$$\sigma_{n,n} = \sigma_{n,T} - \sigma_{n,X}, \qquad (3)$$

the elastic scattering cross section was then obtained at these energies.

Since $\sigma_{n,n}$ is a slowly varying function of A and Z, the shape of the curve recommended by Schmidt[2] was used in extrapolating between the above data. The data between 200 keV and 2 MeV lie somewhat above the recommended curve. This difference is due to the inclusion of the lower levels of $\sigma_{n,n'}$ in the experimental values of the elastic cross section at these energies, and to the uncertainties in the experimental data.

E. Inelastic Scattering Cross Section

We can write

$$\sigma_{n,n'} = \sigma_{n,T} - \sigma_{n,F} - \sigma_{n,n} - \sigma_{n,\gamma} - \sigma_{n,2n} - \sigma_{n,3n}. \qquad (4)$$

Equation 4 was used to establish the general behavior of the total inelastic scattering cross section.

The inelastic scattering cross section is, in reality, a sum of cross sections for excitation of residual nuclear levels. Dzhelepov et al.[14] found levels at 8, 57, 76, 164, 193, 286, 330, 358, 388, 392, 432, 480, and 517 keV. Since the level density becomes quite large above about 300 keV, statistical theory can be applied to the inelastic process for levels above that energy.

The data of Andreev, Cranberg, and Allen combined with the results of Eq. 4, were used to establish the magnitudes of the excitation curves for the levels below 300 keV. The same general shape was assumed for all levels.

Above 5.5 MeV $\sigma_{n,2n}$ becomes nonzero. The cross sections, $\sigma_{n,n'}$ and $\sigma_{n,2n'}$ were taken from the recommended values of Schmidt,[2] modified so that the sum, $\sigma_{n,n'} + \sigma_{n,2n'}$ agreed with the values obtained from Eq. 4. The relative values of the cross sections were determined so that the curves were smoothly continuous at all points.

F. Neutron Energy Distributions for Evaporation Processes

The energy distributions of secondary neutrons from inelastic scattering as given by Andreev[10] at about 1.2 MeV, and Cranberg[11] at 2 MeV, can be fit with an evaporation formula of the form

$$F(E) \quad \frac{E}{T^2} \quad e^{-E/T}, \qquad (5)$$

where T characterizes the nuclear temperature. These fits give nuclear temperatures of about 0.35 and 0.38 MeV, respectively. Zamyatnin et al.[15] measured the neutron energy distribution of all secondary neutrons for an incident neutron energy of 14 MeV. The evaporation component of the spectrum included n,n', n,2n, and n,3n neutrons, as well as the prefission evaporation neutrons. The spectrum of all evaporation neutrons can be fit with Eq. 5 with a temperature of 0.53 MeV.

For the uranium isotopes ^{235}U and ^{238}U, it appears that the energy distribution for all evaporation neutrons can be adequately fit with a single temperature for a given incident neutron energy, in the sense that the overall neutron energy distribution will thereby be correctly described.[16] It is assumed that this also holds for the plutonium isotopes.

Batchelor et al.[17] have found that the nuclear temperatures for both thorium and uranium isotopes increase steadily up to an incident neutron energy of about 4 to 6 MeV, and then level off at approximately constant values. It was assumed that the plutonium isotopes exhibit similar behavior, and the nuclear temperature for ^{239}Pu as a function of incident neutron energy was taken to be as follows:

E (MeV)	T (MeV)
0.55	0.30
1.0	0.35
2.0	0.38
7.	0.53
14.	0.53

The final-state neutron energy distributions for all evaporation processes were then obtained from Eq. 5, using the above temperature specification.

As was noted in the previous section, the level density of ^{239}Pu is high enough to warrant the application of statistical theory to the n,n' process for all excited states whose level energies lie above about 300 keV. From an incident neutron energy of some 300 keV up to 1 MeV, final state neutron energy spectrum is represented by an evaporation spectrum, plus contributions from low-lying levels (with energies below 300 keV) superimposed. Above 1 MeV the evaporation spectrum is completely adequate to describe the neutron energy distribution.

The average contribution of an excited

level to the neutron energy distribution can easily be calculated. If the excitation energy of nuclide A is given by E_i^*, and the energy of the incident neutron in the laboratory system is A, then, on the average, the final neutron energy after an inelastic collision is given by

$$\left\{E_{final}\right\}_i = \frac{1 + A^2\left[1-\left(\frac{A+1}{A}\right)\frac{E_i^*}{E}\right]}{(1 + A)^2} E. \qquad (6)$$

The graph of the partial inelastic cross sections in Fig. 6 at the end of the report gives the relative weights of the energy levels and the statistical model in calculating the final-state energy distribution. It should be noted that, at energies above 300 keV, the statistical model includes an increasing fraction of the excitation curves even for the low-lying levels. This procedure adequately describes the overall neutron energy distribution; in neutronics calculations, that is the only requirement.

G. $\sigma_{n,2n}$ and $\sigma_{n,3n}$

$\sigma_{n,2n}$ was based on Schmidt's recommended curves, as described in Sect. III-E. The n,3n cross section was assumed to be essentially the same as that of ^{235}U, which is given by Parker.[18] The neutron energy distributions are described in Sect. III-F.

H. Number of Prompt Neutrons per Fission

The mean number of prompt neutrons per fission, $\bar{\nu}$, was taken from the compiled data of Stehn et al.[7] and Smith,[19] as well as the thermal data of Critolph[20] and Leonard.[21] A least-squares fit to the data, weighted by relative errors, was made. Assuming successively higher powers of E_n led to the conclusion that a linear fit was the best fit to the data, with the resultant equation,

$$\bar{\nu} = 2.888 + 0.117\ E\ (MeV) \qquad (7)$$

I. Fission Neutron Energy Distribution

Since one neutron from $\sigma_{n,n'f}$ and two from $\sigma_{n,2nf}$ are treated as prefission evaporation neutrons, the prompt neutrons are given by the term

$$\sigma_{n,f} + (\bar{\nu} - 1)\ \sigma_{n,n'f} + (\bar{\nu} - 2)\ \sigma_{n,2nf}.$$

These are distributed according to the final-state prompt fission neutron energy spectrum. A number of measurements of the fission spectrum have been made. The spectrum has been fitted by a Maxwellian distribution:

$$\theta(E) = \frac{2}{\sqrt{\pi}}\ \frac{1}{T^{3/2}}\ E^{\frac{1}{2}}\ e^{-E/T} \qquad (8)$$

and by the well-known sinh law:

$$\theta(E) = \frac{1}{\sqrt{\pi\,\omega\,T_f}}\ e^{-\omega/T_f}\ e^{-E/T_f} \sinh\left(\frac{2\sqrt{\omega\ E}}{T_f}\right) \qquad (9)$$

where T_f and ω are parameters. The errors are generally such as to preclude a clear choice between Eqs. 8 and 9. For consistency the authors have used Eq. 8 to fit all experimental distributions. Barnard et al.[22] give a compilation of values of the nuclear temperature for various isotopes at different incident neutron energies.

Terrell[23] has obtained a function relating the nuclear temperature to $\bar{\nu}$:

$$T\ (E) = A + B\left[\bar{\nu}(E) + 1\right]^{\frac{1}{2}}. \qquad (10)$$

Using the functional relation in Eq. 10, with T (thermal) = 1.38 MeV and T (14 MeV) = 1.59 MeV, a curve of T vs E was obtained. From this curve, the final-state prompt fission neutron energy spectrum was obtained from Eq. 8.

The prefission (evaporation) neutrons from the (n,n'f) and (n,2nf) processes were distributed in energy according to the statistical model, which is described in Sect. III-F.

For ^{239}Pu, Zamyatnin et al.[15] measured the ratio of fission spectrum neutrons to all secondary neutrons, excluding elastic scattering; they obtained 0.72 ± 0.1 for this ratio at 14 MeV. This compares with

0.84 obtained from the recommended curves given in this report.

J. Delayed Neutrons

The delayed neutrons were distributed in energy according to the graph in Fig. 10, with a total delayed neutron fraction, β, of 0.0021 taken from the data given by Keepin[24] and Maksyutenko.[25] The energy distribution was assumed to be the same as for ^{235}U.

K. Angular Distributions

The experimental data on the differential elastic scattering cross section (angular distributions) were fit with the expression

$$\frac{d\sigma_{n,n}}{d\Omega} = \frac{\sigma_{n,n}}{4\pi}\left[1 + \sum_{i=1}^{10} W_i P_i(\mu)\right], \quad (11)$$

where $P_i(\mu)$ are the Legendre polynomials and $\mu = \cos\theta$. There are only a few experimental points, primarily those of Cranberg[11] and Allen.[12] The values of W_i for ^{239}Pu were then taken to be the same as for ^{238}U, as given by the authors.[16] As can be seen from the graphs in Fig. 9, they are consistent with the experimental points for ^{239}Pu.

Nonelastic reactions were assumed to have isotropic angular distributions.

L. Recommended Curves

The cross-section curves for ^{239}Pu, along with the Legendre coefficients for $\frac{d\sigma_{n,n}}{d\Omega}$, are shown in Figs. 1 through 10.

The experimental data from the above references are also plotted on the graphs. No attempt is made to identify the sources of the individual points. The cross sections are tabulated in Table I.

IV. PLUTONIUM-240

A. Total Cross Section

There are no data on the total cross section for ^{240}Pu above 100 eV. Therefore, the total cross section was determined entirely by the sum of the partial cross sections.

B. Fission Cross Section

In addition to the compilations of Hughes and Schwartz and Stehn et al., measurements have been reported by Nesterov and Smirenkin,[26] Ferguson and Pattenden,[4] Zamyatnin,[27] and Perkin et al.[28]

The threshold for fission is not well established. Early data given by Hughes and Schwartz indicated a threshold near 0.1 MeV. More recent laboratory experiments have found nonzero measurements as low as 23 keV, with considerable scatter in the data up to 150 keV.

Very recently the technique of using the neutron flux from underground nuclear devices has been used to measure cross sections; in particular the fission cross section of ^{240}Pu has been measured by Byers et al.[29] Although the scatter of data is large, there appears to be a nonzero fission cross section down to about 1 keV. An average of these measurements was taken from around 100 keV to 1 keV.

Above this range, the fission cross section is well established up to 8 MeV. Between 8 and 14 MeV, the ^{239}Pu fission cross section was used to establish the shape of the curve, with the data at 14 MeV providing the normalization.

The (n,n'f) cross section has a threshold at 5.5 MeV, with the total fission cross section exhibiting the characteristic sharp increase at this point. Above 5.5 MeV, $\sigma_{n,f}$ was assumed to be a constant. The (n,2nf) reaction threshold was assumed to be 10.5 MeV, with $\sigma_{n,n'f}$ taken to be a constant above this energy.

C. Radiative Capture Cross Section

No data on $\sigma_{n,\gamma}$ have been reported above 1 keV. Hamilton[30] has given semiempirial calculations of $\sigma_{n,\gamma}$ at decade intervals from 1 keV to 1 MeV, and Buckingham et al.[31] and Douglas[32] give recommended curves for $\sigma_{n,\gamma}$ up to 15 MeV.

Table I

CROSS SECTIONS FOR ^{239}Pu IN BARNS

Energy (MeV)	$\sigma_{n,F}$	$\sigma_{n,n}$	$\sigma_{n,\gamma}$	$\sigma_{n,n'}$	$\sigma_{n,2n}$	$\sigma_{n,3n}$
0.0010	5.80	14.00	4.40	-	-	-
0.0015	3.11	13.65	2.67	-	-	-
0.0020	1.75	13.50	1.30	-	-	-
0.0025	2.62	13.20	1.87	-	-	-
0.0030	2.80	13.10	1.95	-	-	-
0.0040	2.65	12.83	1.81	-	-	-
0.0050	2.48	12.63	1.63	-	-	-
0.0060	2.33	12.40	1.42	-	-	-
0.0070	2.22	12.35	1.26	-	-	-
0.0080	2.10	12.32	1.14	-	-	-
0.0090	2.01	12.30	1.07	0.056	-	-
0.010	1.91	12.20	1.01	0.095	-	-
0.015	1.63	12.10	0.830	0.165	-	-
0.020	1.52	11.91	0.730	0.199	-	-
0.025	1.48	11.70	0.654	0.217	-	-
0.030	1.45	11.30	0.590	0.226	-	-
0.040	1.44	10.91	0.465	0.237	-	-
0.050	1.44	10.70	0.363	0.239	-	-
0.060	1.44	10.35	0.292	0.248	-	-
0.070	1.47	10.10	0.270	0.266	-	-
0.080	1.48	10.00	0.253	0.264	-	-
0.090	1.49	9.90	0.247	0.280	-	-
0.10	1.49	9.77	0.241	0.296	-	-
0.15	1.51	9.00	0.219	0.379	-	-
0.20	1.52	8.39	0.198	0.453	-	-
0.25	1.52	7.85	0.179	0.481	-	-
0.30	1.53	7.35	0.164	0.521	-	-
0.40	1.57	6.63	0.143	0.574	-	-
0.50	1.57	6.05	0.123	0.652	-	-
0.60	1.57	5.65	0.108	0.71	-	-
0.70	1.58	5.27	0.083	0.78	-	-
0.80	1.60	4.94	0.068	0.86	-	-
0.90	1.62	4.71	0.056	0.90	-	-
1.0	1.65	4.59	0.047	0.94	-	-
1.5	1.86	3.98	0.026	1.19	-	-
2.0	1.95	3.89	0.019	1.43	-	-
2.5	1.92	4.12	0.014	1.59	-	-
3.0	1.90	4.40	0.011	1.63	-	-
3.5	1.89	4.47	0.010	1.66	-	-
4.0	1.88	4.50	-	1.64	-	-
4.5	1.82	4.49	-	1.64	-	-
5.0	1.82	4.48	-	1.62	-	-
5.5	1.82	4.47	-	1.50	-	-
6.0	1.87	4.41	-	1.29	0.030	-
6.5	1.97	4.33	-	0.86	0.160	-
7.0	2.10	4.15	-	0.572	0.268	-
7.5	2.21	3.87	-	0.410	0.309	-
8.0	2.30	3.67	-	0.307	0.337	-
8.5	2.35	3.53	-	0.242	0.360	-
9.0	2.40	3.37	-	0.202	0.378	-

Table I (Continued)

Energy (MeV)	$\sigma_{n,F}$	$\sigma_{n,n}$	$\sigma_{n,\gamma}$	$\sigma_{n,n'}$	$\sigma_{n,2n}$	$\sigma_{n,3n}$
9.5	2.41	3.25	-	0.184	0.396	-
10.0	2.41	3.18	-	0.176	0.400	-
10.5	2.42	3.12	-	0.162	0.389	-
11.0	2.44	3.07	-	0.149	0.343	-
11.5	2.47	3.04	-	0.132	0.305	-
12.0	2.50	3.03	-	0.123	0.247	-
12.5	2.51	3.03	-	0.117	0.198	-
13.0	2.53	3.03	-	0.111	0.160	-
13.5	2.54	3.03	-	0.106	0.110	0.024
14.0	2.55	3.03	-	0.102	0.061	0.055

The $\sigma_{n,\gamma}$ curve was chosen to connect Hamilton's values smoothly, going to 10 mb at 14 MeV.

D. Elastic Scattering Cross Section

No data exist for $\sigma_{n,n}$. Since elastic scattering is only slightly dependent on A and Z, the ^{239}Pu curve was used, along with the recommended values of Buckingham et al.[31] and Douglas,[32] to establish $\sigma_{n,n}$ for ^{240}Pu.

E. Inelastic Scattering Cross Section

The excited levels of ^{240}Pu have been determined by Bunker et al.,[33] Bjornholm et al.,[34] and Lederer.[35] Since the level density becomes large above about 900 keV, statistical theory should be applicable above that energy. The procedure for determining the partial cross sections for the individual levels is the same as that used for ^{239}Pu, described in Sect. III-E. The magnitude of the total inelastic cross section was chosen to follow generally the recommendation of Buckingham et al.

F. Neutron Energy Distributions for Evaporation Processes

As was described in Sect. III-F, it is assumed that the final-state neutron energy distributions from all inelastic processes can be represented by Eq. 5, with a single curve of temperature versus incident neutron energy. No experimental measurements of the evaporation spectra have been reported.

Between about 900 keV and 1.5 MeV, the neutron energy spectrum was represented by the evaporation spectrum plus contributions from the low-lying excited states, as described in Sect. III-F. Above 1.5 MeV, the energy spectrum was represented entirely by the evaporation spectrum. The behavior of T vs. E for ^{240}Pu was assumed to be similar to that for ^{239}Pu, giving the following table:

E (MeV)	T (MeV)
0.8	0.30
1.5	0.32
7	0.45
14	0.45

G. $\sigma_{n,2n}$ and $\sigma_{n,3n}$.

No measurements are available on these processes. The recommended values are the same as those given for ^{239}Pu (Sect. III-G), assuming that the dependence on A is very small.

H. Number of Prompt Neutrons per Fission

Only three measured points of the induced fission of ^{240}Pu have been reported. Kuzminov[36] gives values at 3.6 and 15 MeV, while Barton et al.[37] have inferred a value from a fission spectrum centered around 2 MeV. These points were fitted with a function linear in incident neutron energy, for energies above the fission threshold:

$$\bar{\nu}(E) = 3.118 + 0.089\ E\ (\text{MeV}). \quad (12)$$

I. Fission Neutron Energy Distribution

The direct fission neutrons are distributed according to the final-state prompt fission neutron energy spectrum, which was assumed to follow Eq. 8. The nuclear temperatures were taken from the recommended values of Douglas,[32] which follow the functional form of Eq. 10, with T (thermal) 1.34 MeV and T (14 MeV) = 1.48 MeV.

J. Delayed Neutrons

The delayed neutron fraction, β, is given by Keepin[24] to be 0.0027. This fraction is distributed in energy in the same fashion as those from ^{239}Pu, as given in Fig. 10.

K. Angular Distributions

The differential elastic scattering cross section (angular distribution) was assumed to have the same angular dependence as that for ^{239}Pu. The Legendre polynomial coefficients from Eq. 11 are given for both ^{239}Pu and ^{240}Pu in Fig. 9.

Nonelastic reactions were assumed to have isotropic angular distributions.

L. Recommended Curves

The cross-section curves for ^{240}Pu are given in Figs. 11 through 18. The experimental data from the above references are also plotted on the graphs. The cross sections are tabulated in Table II.

Table II

CROSS SECTIONS FOR ^{240}Pu IN BARNS

Energy (MeV)	$\sigma_{n,F}$	$\sigma_{n,n}$	$\sigma_{n,\gamma}$	$\sigma_{n,n'}$	$\sigma_{n,2n}$	$\sigma_{n,3n}$
0.0010	0.010	10.0	6.70	-	-	-
0.0015	0.017	9.94	4.42	-	-	-
0.0020	0.025	9.90	3.34	-	-	-
0.0025	0.031	9.86	2.75	-	-	-
0.0030	0.037	9.83	2.33	-	-	-
0.0040	0.047	9.79	1.83	-	-	-
0.0050	0.054	9.75	1.52	-	-	-
0.0060	0.061	9.72	1.31	-	-	-
0.0070	0.068	9.69	1.19	-	-	-
0.0080	0.073	9.66	1.08	-	-	-
0.0090	0.078	9.63	1.00	-	-	-
0.010	0.082	9.60	0.94	-	-	-
0.015	0.091	9.55	0.772	-	-	-
0.020	0.094	9.50	0.689	-	-	-
0.025	0.095	9.45	0.645	-	-	-
0.030	0.095	9.40	0.602	-	-	-
0.040	0.095	9.34	0.559	-	-	-
0.050	0.095	9.28	0.521	0.013	-	-
0.060	0.095	9.22	0.495	0.024	-	-
0.070	0.095	9.17	0.468	0.036	-	-
0.080	0.095	9.11	0.442	0.050	-	-
0.090	0.095	9.06	0.420	0.063	-	-
0.10	0.095	9.00	0.400	0.075	-	-
0.15	0.095	8.55	0.323	0.115	-	-
0.20	0.095	8.12	0.277	0.169	-	-
0.25	0.117	7.72	0.241	0.226	-	-
0.30	0.141	7.32	0.216	0.313	-	-
0.40	0.210	6.65	0.179	0.312	-	-
0.50	0.390	6.08	0.153	0.162	-	-
0.60	0.64	5.72	0.137	0.086	-	-

Table II (Continued)

Energy (MeV)	$\sigma_{n,F}$	$\sigma_{n,n}$	$\sigma_{n,\gamma}$	$\sigma_{n,n'}$	$\sigma_{n,2n}$	$\sigma_{n,3n}$
0.70	0.85	5.38	0.123	0.208	-	-
0.80	1.11	5.09	0.114	0.367	-	-
0.90	1.41	4.83	0.107	0.425	-	-
1.0	1.69	4.63	0.100	0.485	-	-
1.5	1.62	4.08	0.076	1.66	-	-
2.0	1.67	4.19	0.061	1.72	-	-
2.5	1.68	4.41	0.051	1.72	-	-
3.0	1.67	4.66	0.043	1.72	-	-
3.5	1.67	4.72	0.038	1.72	-	-
4.0	1.62	4.74	0.034	1.72	-	-
4.5	1.53	4.75	0.030	1.72	-	-
5.0	1.50	4.74	0.027	1.72	-	-
5.5	1.53	4.72	0.025	1.69	-	-
6.0	1.66	4.70	0.023	1.55	0.030	-
6.5	1.83	4.67	0.021	1.40	0.160	-
7.0	1.96	4.57	0.020	1.20	0.268	-
7.5	2.04	4.33	0.019	0.82	0.308	-
8.0	2.11	4.00	0.018	0.57	0.337	-
8.5	2.16	3.73	0.017	0.378	0.360	-
9.0	2.20	3.49	0.016	0.262	0.378	-
9.5	2.21	3.33	0.015	0.183	0.396	-
10.0	2.21	3.21	0.014	0.132	0.400	-
10.5	2.22	3.14	0.013	0.113	0.389	-
11.0	2.25	3.12	0.013	0.108	0.343	-
11.5	2.31	3.11	0.012	0.105	0.305	-
12.0	2.36	3.10	0.012	0.103	0.247	-
12.5	2.41	3.09	0.011	0.102	0.198	-
13.0	2.44	3.08	0.011	0.101	0.160	-
13.5	2.47	3.07	0.010	0.100	0.110	0.024
14.0	2.49	3.07	0.010	0.100	0.061	0.055

ACKNOWLEDGMENTS

The authors are very happy to acknowledge the help of C. P. Cadenhead and K. F. Famularo of LASL Group W-4 in providing many suggestions and critical evaluations of the results of this effort. Also, the authors would like to acknowledge the tireless asistance of Beverly Wellnitz and Nora Sanchez of W-4 in the physical preparation of this report.

REFERENCES

1. C. C. Cremer, R. E. Hunter, and J.-J. H. Berlijn, "Comparison of Calculations with Integral Experiments for Plutonium and Uranium Critical Assemblies," LA-3529 (1968).
2. J. J. Schmidt, "Neutron Cross Sections for Fast Reactor Materials," KFK-120 (EANDC-E-35U), (1962).
3. D. J. Hughes and R. B. Schwartz, "Neutron Cross Sections," BNL-325, 2nd Ed. (1958).
4. A. T. G. Ferguson and N. J. Pattenden, "Neutron Cross Section Measurements at Harwell in Support of the U. K. Fast Reactor Programme," ANL-6792, p. 11 (1964).
5. G. D. James, "The Fission Cross Section of Pu^{239} from 1 keV to 160 keV,"

References (Continued)

Symposium on the Absolute Determination of Neutron Flux in the Energy Range 1-100 keV, St. John.s College, Oxford, Sept. 10-13, 1963, EANDC-33U (Paper a) (1963); "Fission Cross Section Measurements on Pu^{239}, Pu^{241}, U^{232} and a Search for Fission Components in Pu^{238} Resonances," IAEA Preprint No. SM-60/15 (1965).

6. P. H. White, J. C. Hodgkinson, and G. C. Wall, "Measurement of Fission Cross-Sections for Neutrons of Energies in the Range 40-500 keV," Proc. Symp. Phys. Chem. Fission, Salzburg, 22-26 March 1965, p. 219, IAEA, Vienna (1965).
7. J. R. Stehn, M. D. Goldberg, R. Wiener-Chasman, S. F. Mughabghab, B. A. Magurno, and V. M. May, "Neutron Cross Sections," BNL-325, 2nd Ed., Supp. No. 2 (1965).
8. A. C. Douglas and J. F. Barry, "Neutron Cross Sections of Pu^{239} in the Energy Range 1 keV to 15 MeV," AWRE-0-79/64 (1964).
9. D. Okrent and F. W. Thalgott, "The Physics of Plutonium in Fast Reactors," HW-75007, p. 14.1 (1964).
10. V. N. Andreev, "Inelastic Scattering of Neutrons of the Fission Spectrum and Neutrons with an Energy of 0.9 MeV in U^{235} and Pu^{239}," Soviet Progress in Neutron Physics, Consultants Bureau Enterprizes, New York: 1963, p. 211.
11. L. A. Cranberg, "Neutron Scattering by U^{235}, Pu^{239} and U^{238}," LA-2177 (1959).
12. R. C. Allen, "The Interaction of 0.15 to 1.0 MeV Neutrons with U-238, U-235, and Pu-239," Nucl. Sci. Eng. 2, 787 (1957).
13. Yu. G. Degtyarev, "Cross Sections for Neutron Inelastic Interactions with ^{7}Li, ^{12}C, ^{12}Al, ^{56}Fe, Cu, Pb, ^{235}U, ^{238}U, and ^{239}Pu," At. Energ. (USSR) 19, 456 (1965).
14. B. S. Dzhelepov, R. B. Ivanov, V. G. Nedovesov, and V. P. Chechev, "Alpha Decay of Curium Isotopes," Zh. Eksperim. i. Teor. Fiz. 45, 1360 (1963); JETP 18, 937 (1964).
15. Yu. S. Zamyatnin, I. N. Safina, E. K. Gutnikova, and N. I. Ivanova, "Spectra of Neutrons Produced by 14 MeV Neutrons in Fissile Materials," At. Energ. (USSR) 4, 337 (1958); Soviet J. At. Energy 4, 443 (1958).
16. J.-J. H. Berlijn, C. C. Cremer, and R. E. Hunter, "Neutron Cross Sections for ^{235}U and ^{238}U in the Energy Range 1 keV - 14 MeV," LA-3527 (1968).
17. R. Batchelor, W. B. Gilboy, and J. H. Towle, "Neutron Interactions with U^{238} and Th^{232} in the Energy Region 1.6 MeV to 7 MeV," EANDC(UK) 48S (1964); also Nucl. Phys. 65, 236 (1965).
18. K. Parker, "Neutron Cross Sections of U^{235} and U^{238} in the Energy Range 1 keV - 15 MeV," AWRE-0-82/63 (1963).
19. A. B. Smith, "Recent Changes in Heavy Element Cross Sections," ANL-6792, p. 31 (1964).
20. E. Critolph, "Effective Cross Sections for U^{235} and Pu^{239}," CRRP-1191 (1964).
21. B. R. Leonard, Jr., "Plutonium Physics: Contribution to Plutonium Handbook," HW-72947 (1963).
22. E. Barnard, A. T. G. Ferguson, W. R. McMurray, and I. J. VanHeerden, "Time-of-Flight Measurements of Neutron Spectra from the Fission of U^{235}, U^{238}, and Pu^{239}," Nucl. Phys. 71, 228 (1965).
23. J. Terrell, "Fission Neutron Spectra and Nuclear Temperatures," Phys. Rev. 113, 527 (1959).
24. G. R. Keepin, "Basic Kinetics Data and Neutron-Effectiveness Calculations," TID-7662, p. 334 (1964).
25. B. P. Maksyutenko, "Delayed Neutrons from Pu^{239}," At. Energ. (USSR) 15, 157 (1964); Soviet J. At. Energy 15, 848 (1964).
26. V. G. Nesterov and G. N. Smirenkin, "Fission Cross Section of Pu ^{240} by Fast Neutrons," Zh. Eksperim, i Teor. Fiz. 35, 532 (1958); JETP 8, 367 (1959).

References (Continued)

27. Yu. S. Zamyatnin, "Cross Sections for Fission Induced by Fast Neutrons," At. Energy (USSR) Supplement No. 1, 27 (1957); Physics of Fission, p. 21 (1957).
28. J. L. Perkin, P. H. White, P. Fieldhouse, E. J. Axton, P. Cross, and J. C. Robertson, "The Fission Cross Sections of U^{233}, U^{234}, U^{236}, Np^{237}, Pu^{239}, Pu^{240}, and Pu^{241} for 24 keV Neutrons," J. Nucl. Energy 19, 423 (1965).
29. D. H. Byers, B. C. Diven, and M. G. Silbert, "Capture and Fission Cross Sections of Pu^{240}," Conf. Neutron Cross Section Technology, Washington, D. C., Mar. 22-24, 1966, Paper F-5 (1966).
30. R. A. H. Hamilton, "Neutron Capture Cross Sections for Uranium and Plutonium Isotopes in the Energy Range 1 keV - 1 MeV," AWRE-O-38/64 (1964).
31. B. R. S. Buckingham, K. Parker, and E. D. Pendlebury, "Neutron Cross Sections of Selected Elements and Isotopes for Use in Neutronics Calculations in the Energy Range 0.025 ev-15 MeV," AWRE-O-28/60 (1961).
32. A. C. Douglas, "Neutron Cross Sections of Pu-240 in the Energy Range 1 keV to 15 MeV," AWRE-O-91/64 (1964).
33. M. E. Bunker, B. J. Dropesky, J. D. Knight, J. W. Starner, and B. Warren, "Decay of U^{240} and 7.3 Min. Np^{240}," Phys. Rev. 116, 143 (1959).
34. S. Bjornholm, M. Lederer, F. Asaro, and I. Perlman, "Alpha Decay to Vibrational States," Phys. Rev. 130, 2000 (1963).
35. C. M. Lederer, "The Structure of Heavy Nuclei: A Study of Very Weak Alpha Branching," UCRL-11028 (1963).
36. B. D. Kuzminov, "Average Number of Prompt Neutrons in Fission of Pu^{240} by Neutrons with Energy of 3.6 and 15 MeV," AEC-tr-4710 (1960).
37. D. M. Barton, W. Bernard, and G. E. Hansen, "Critical Masses of Composites of Oy and $Pu^{239-240}$ in Flattop Geometry," LAMS-2489 (1960).

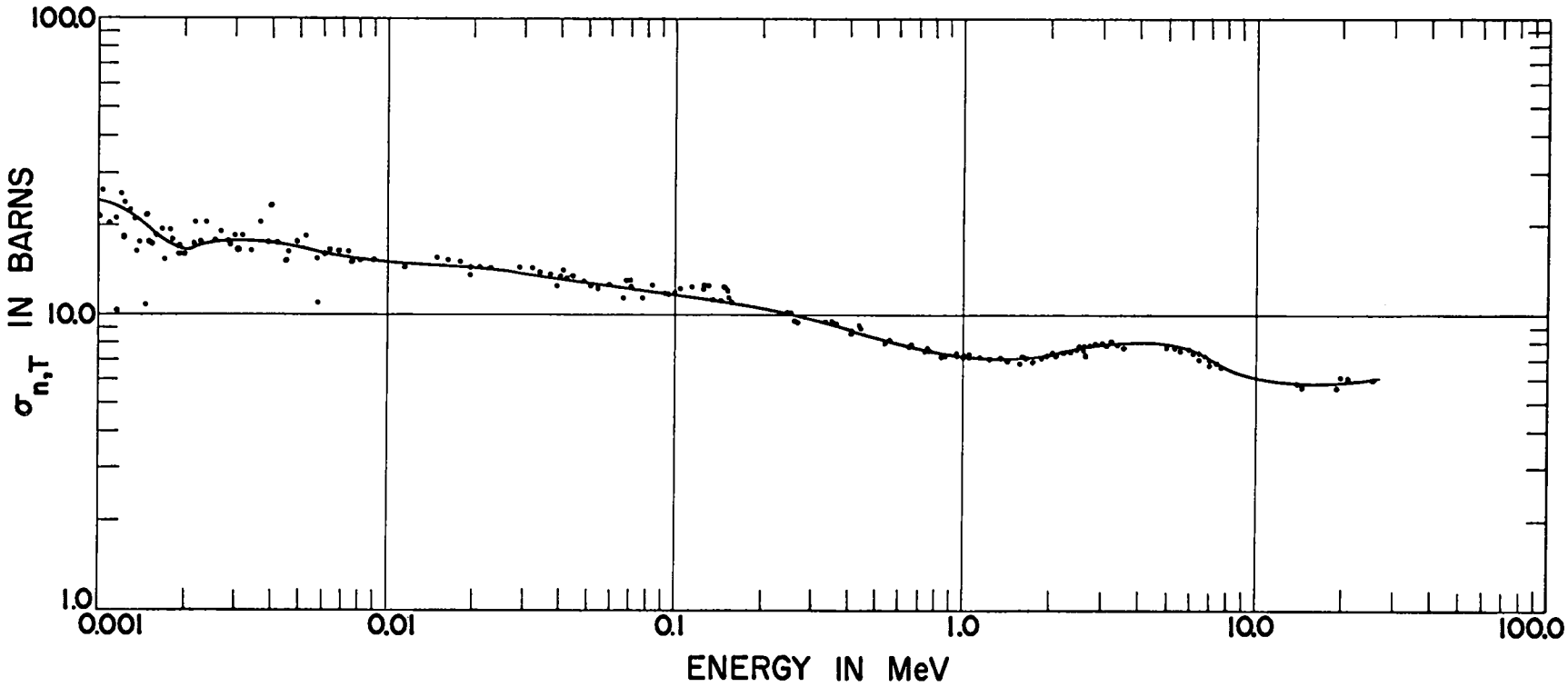

Fig. 1. Total cross section for ^{239}Pu.

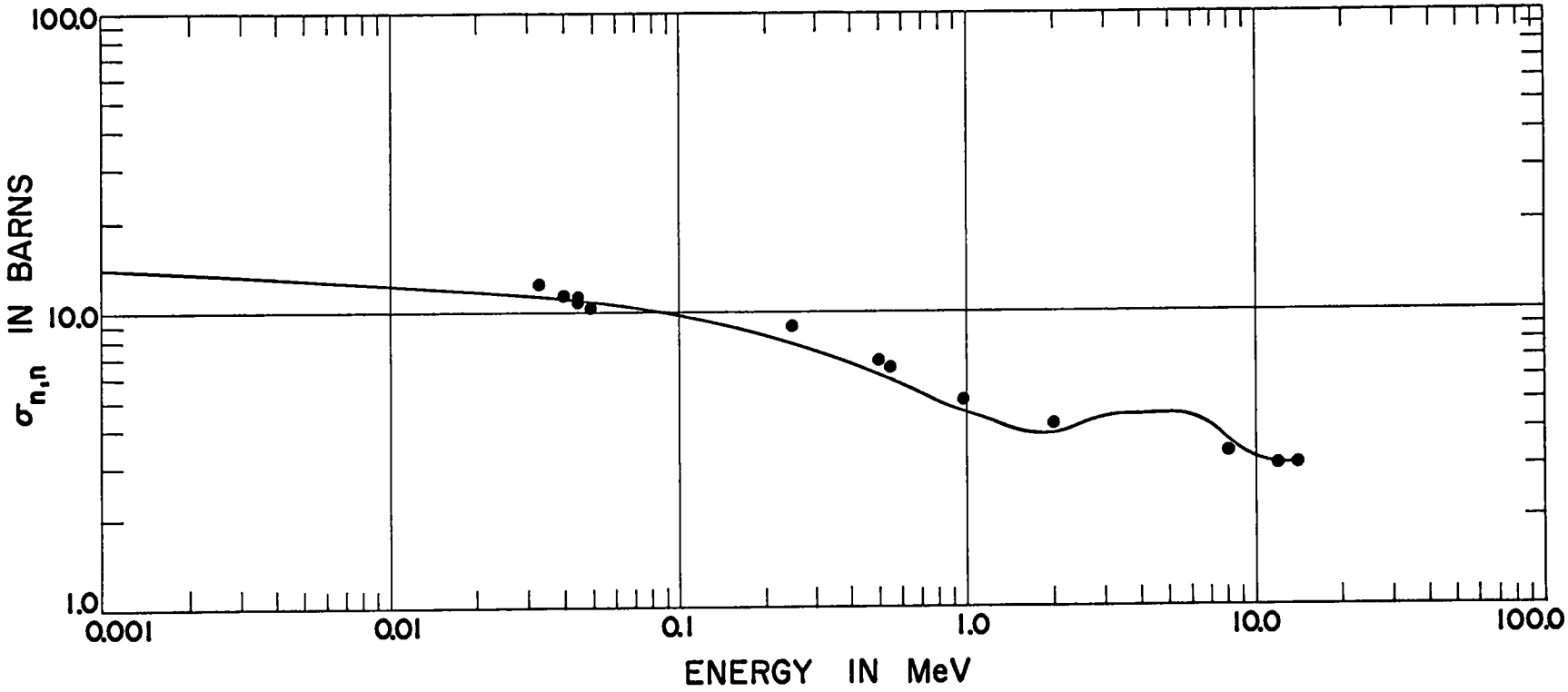

Fig. 2. Elastic scattering cross section for ^{239}Pu.

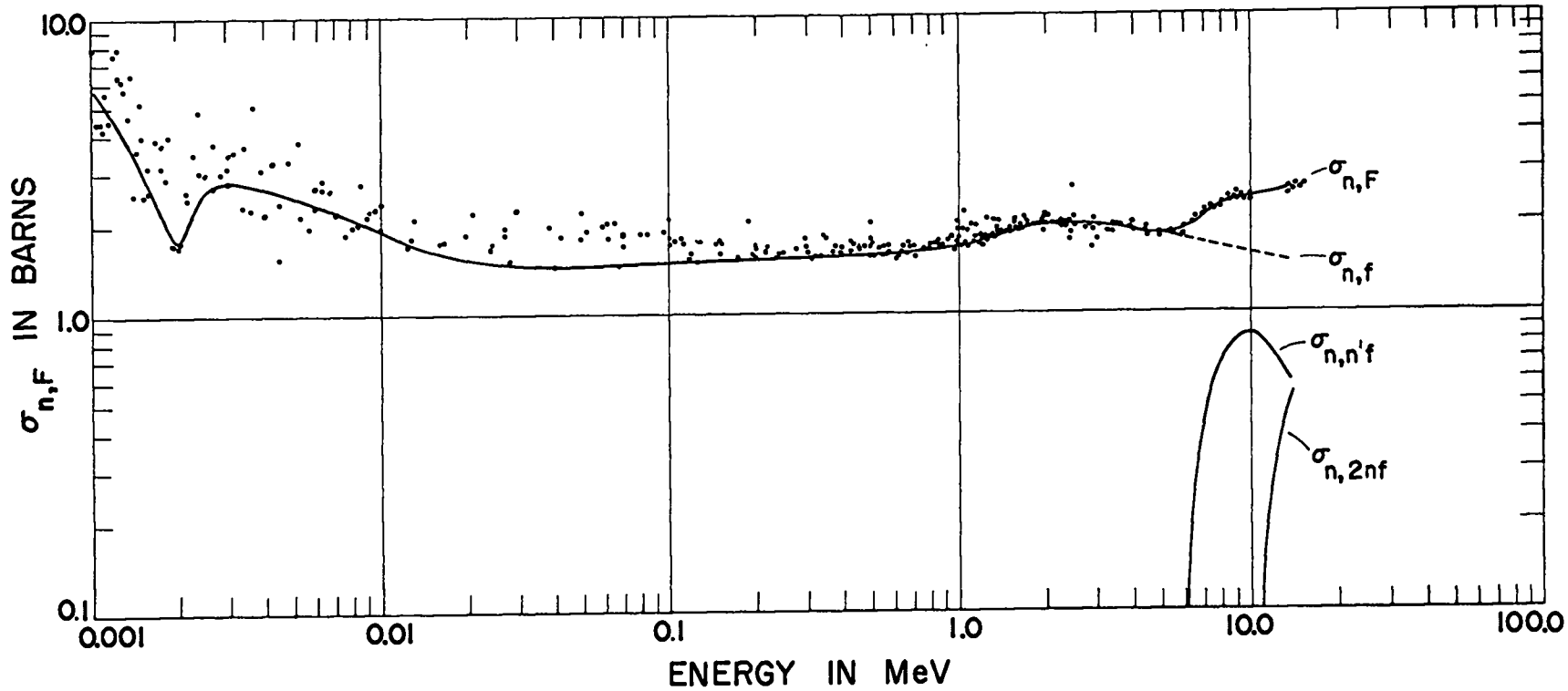

Fig. 3. Fission cross section for ^{239}Pu.

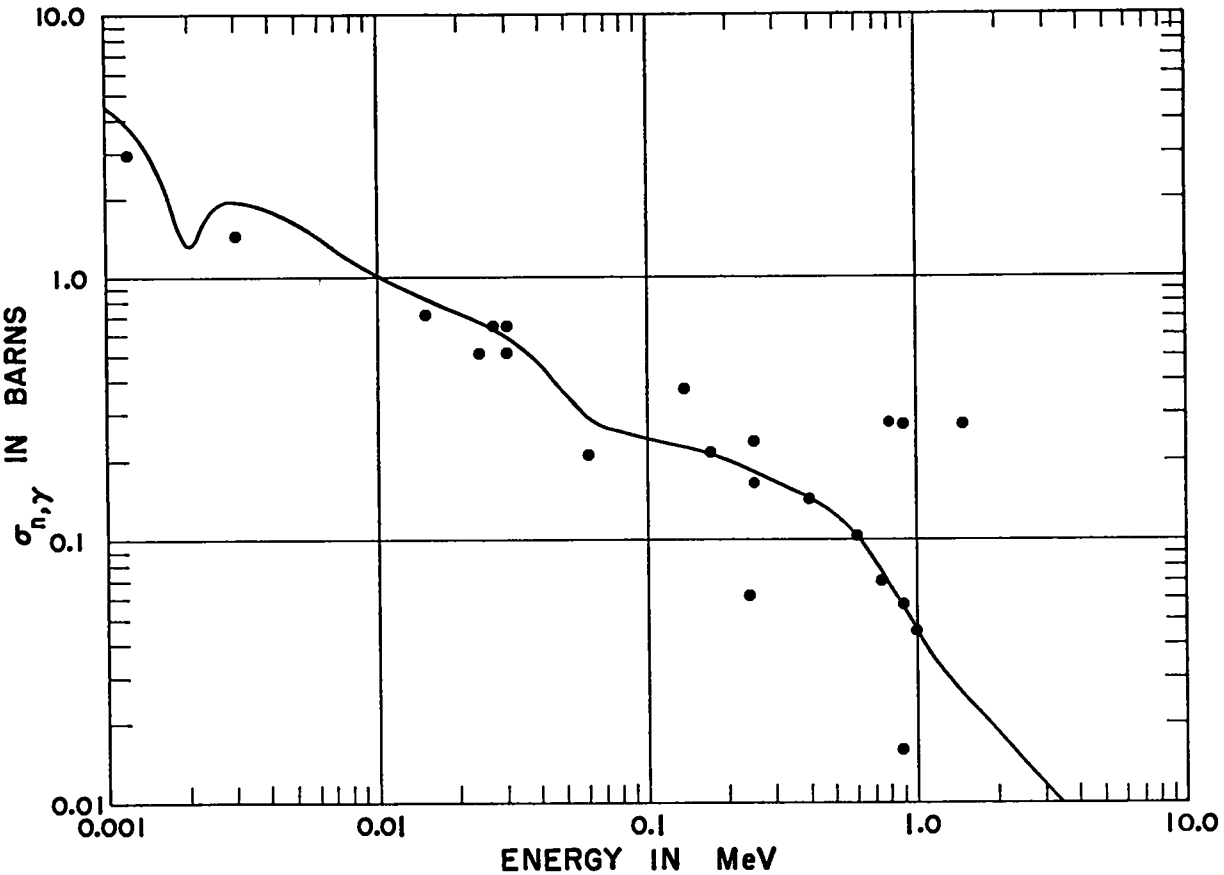

Fig. 4. Radiative capture cross section for ^{239}Pu.

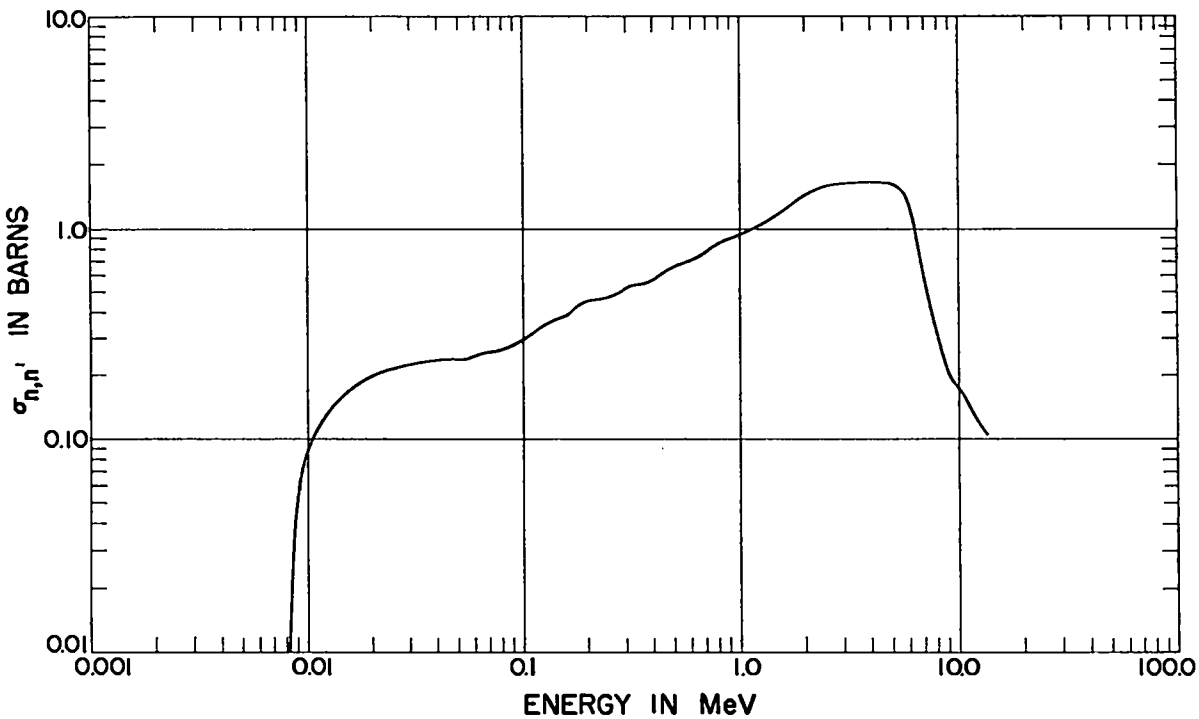

Fig. 5. Inelastic scattering cross section for ^{239}Pu.

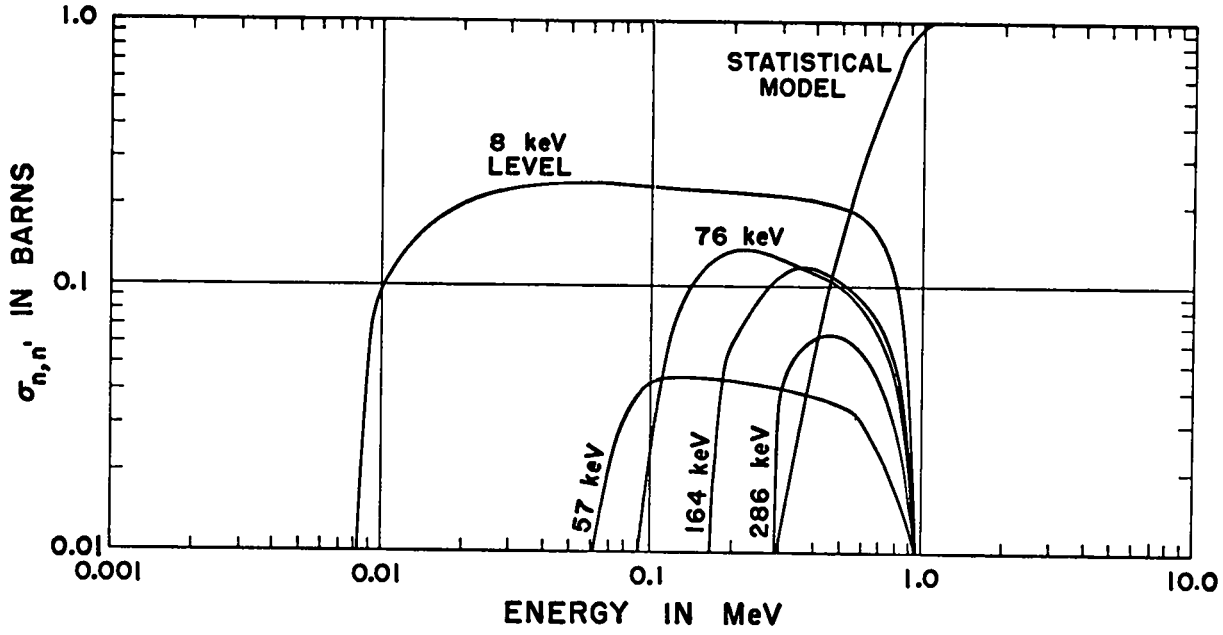

Fig. 6. Partial inelastic scattering cross sections for ^{239}Pu.

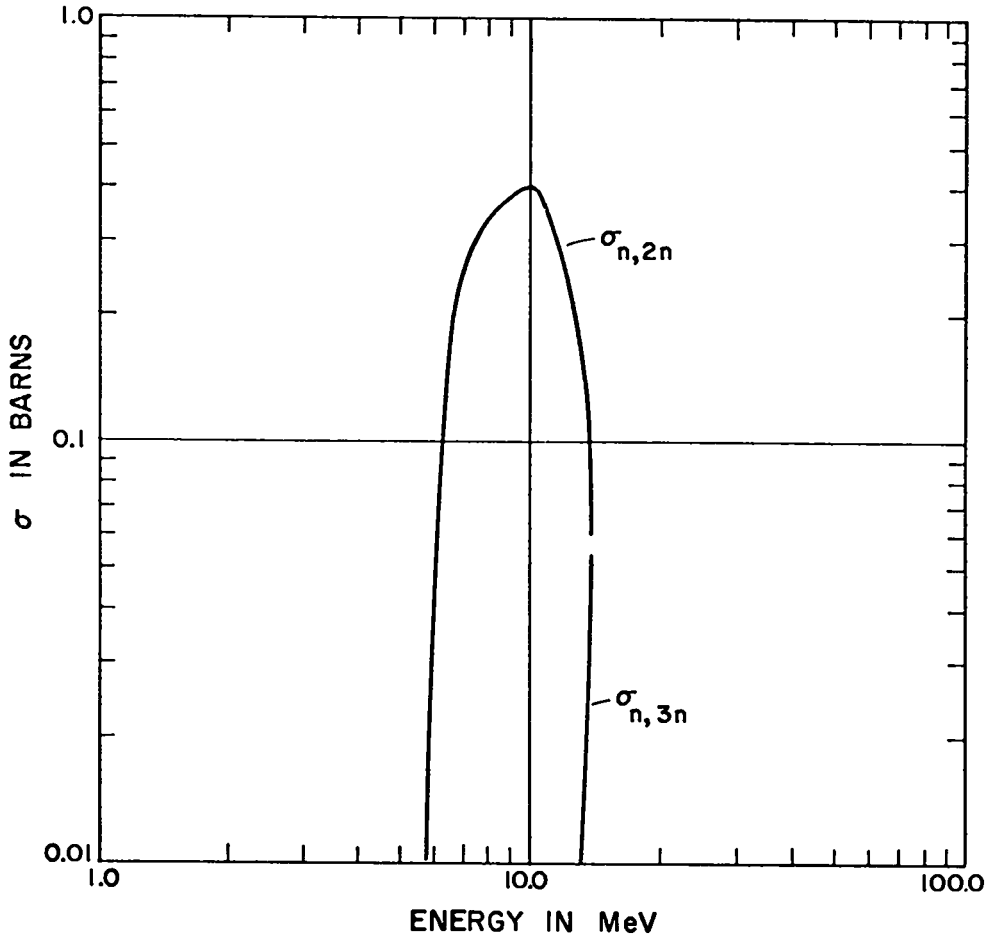

Fig. 7. $\sigma_{n,2n}$ and $\sigma_{n,3n}$ for ^{239}Pu.

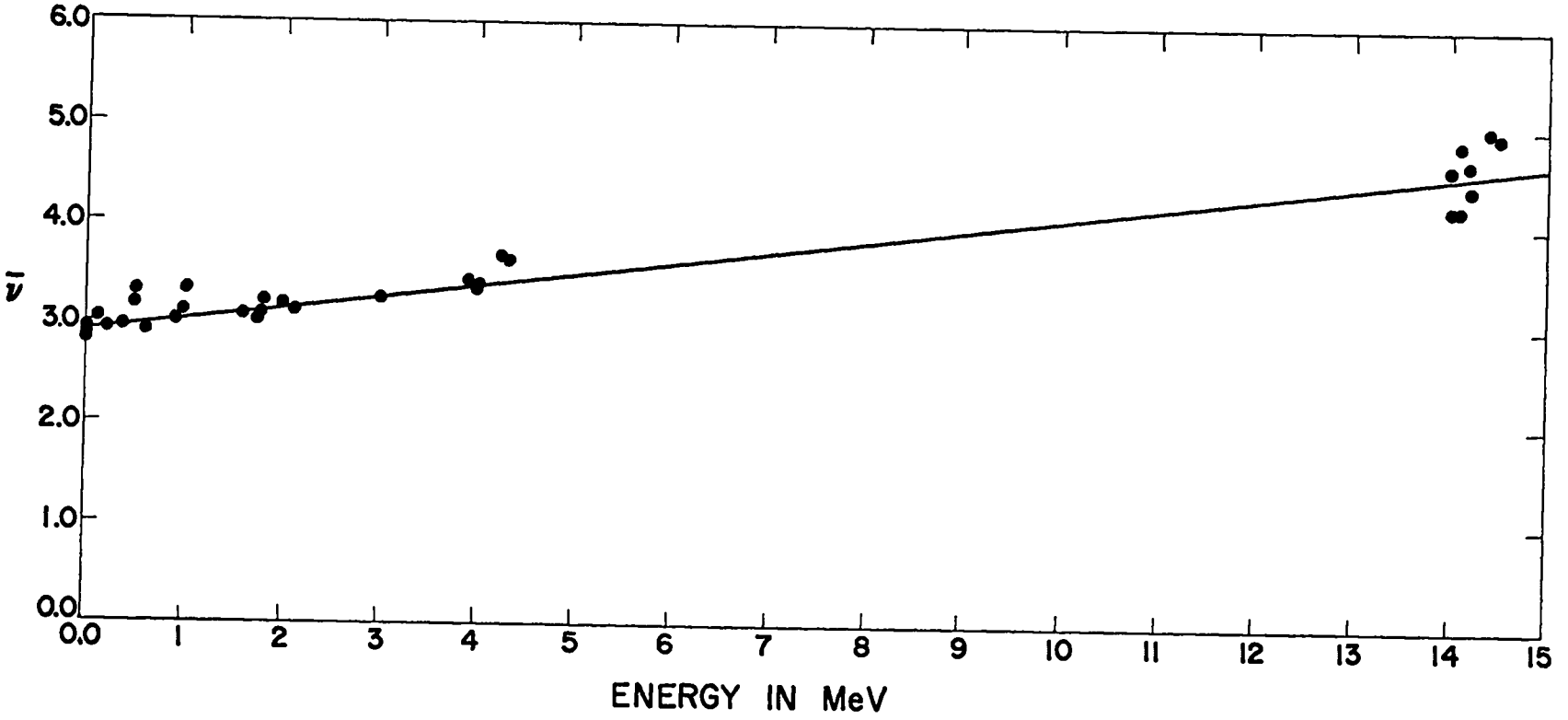

Fig. 8. Mean number of neutrons per fission for ^{239}Pu.

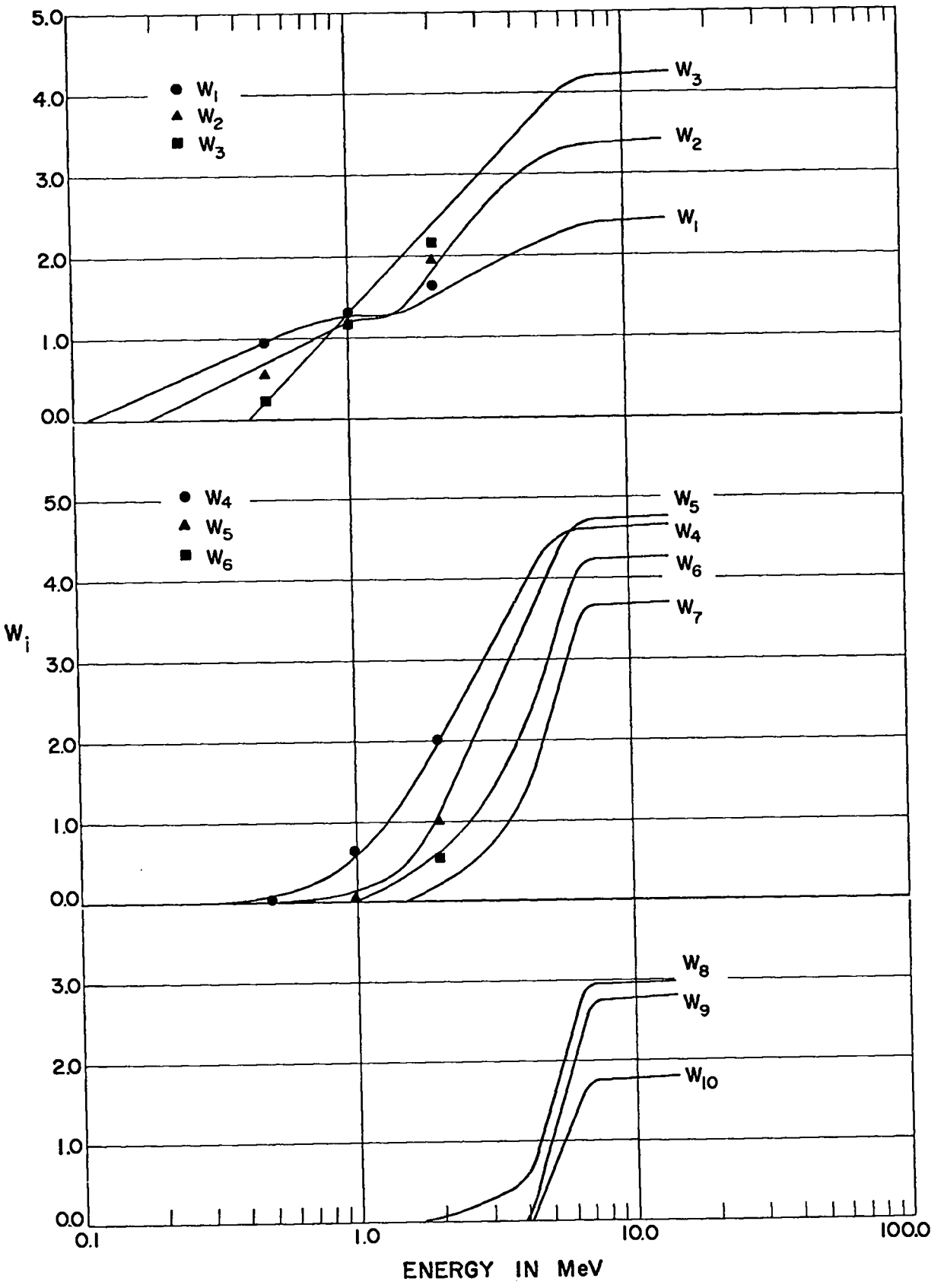

Fig. 9. Elastic scattering Legendre coefficients for ^{239}Pu and ^{240}Pu.

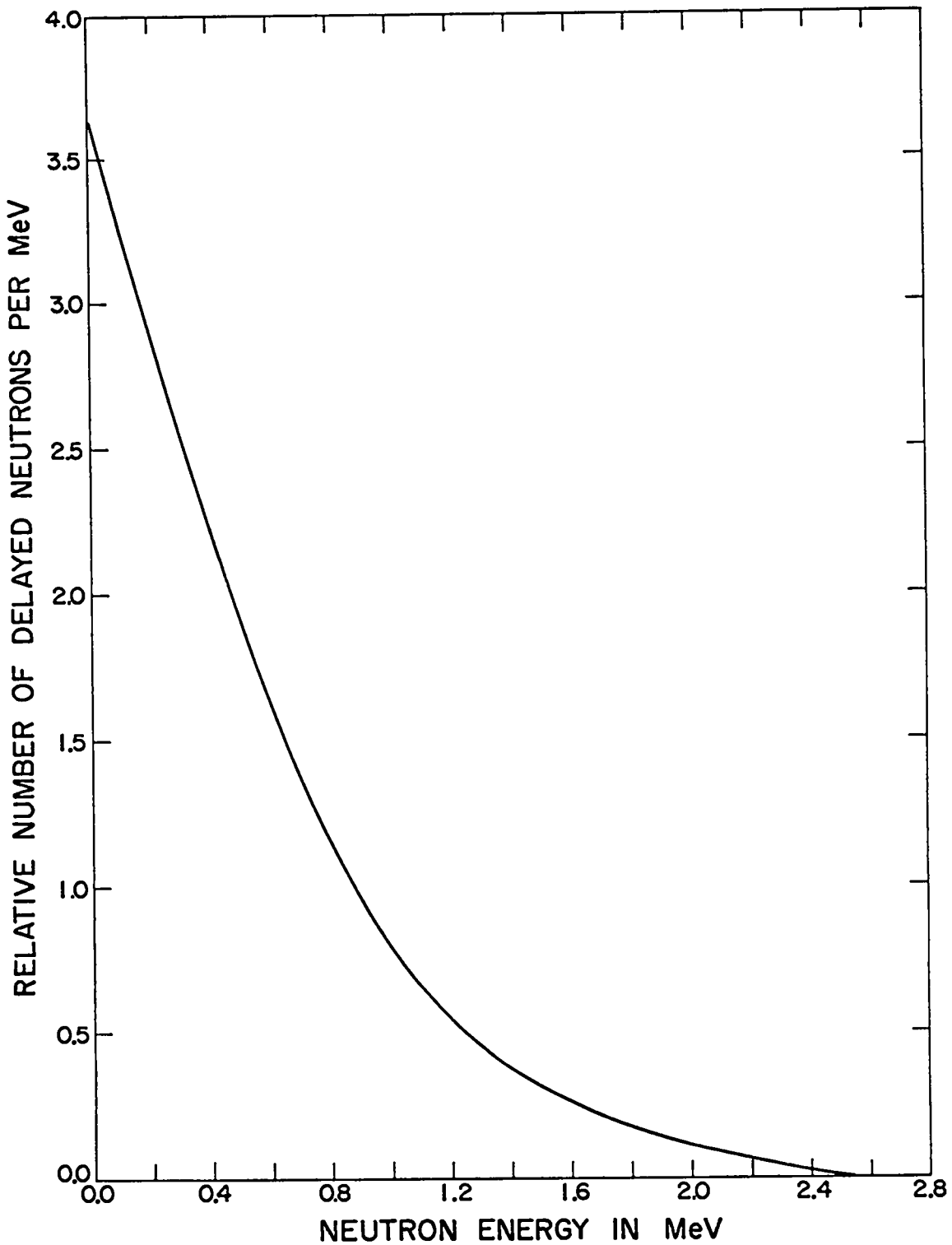

Fig. 10. Delayed neutron energy distribution for ^{239}Pu and ^{240}Pu.

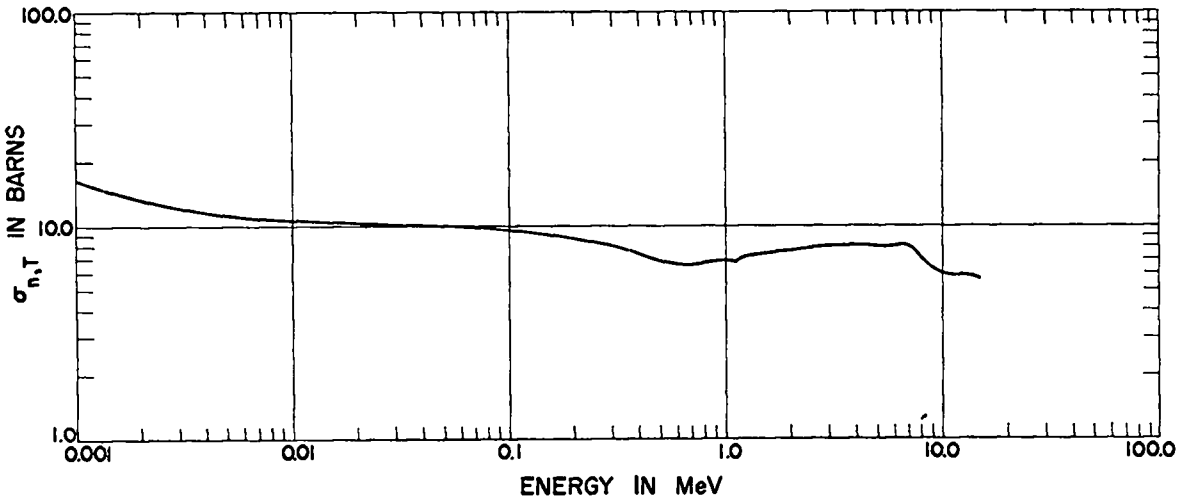

Fig. 11. Total cross section for ^{240}Pu.

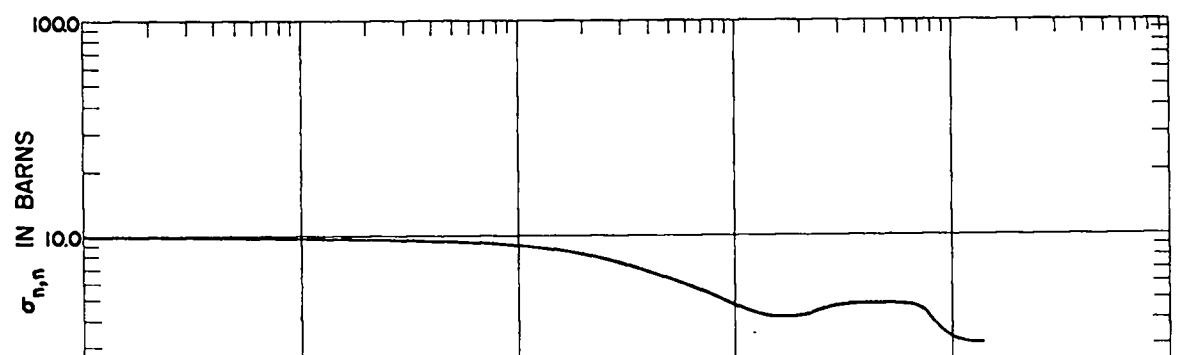

Fig. 12. Elastic scattering cross section for ^{240}Pu.

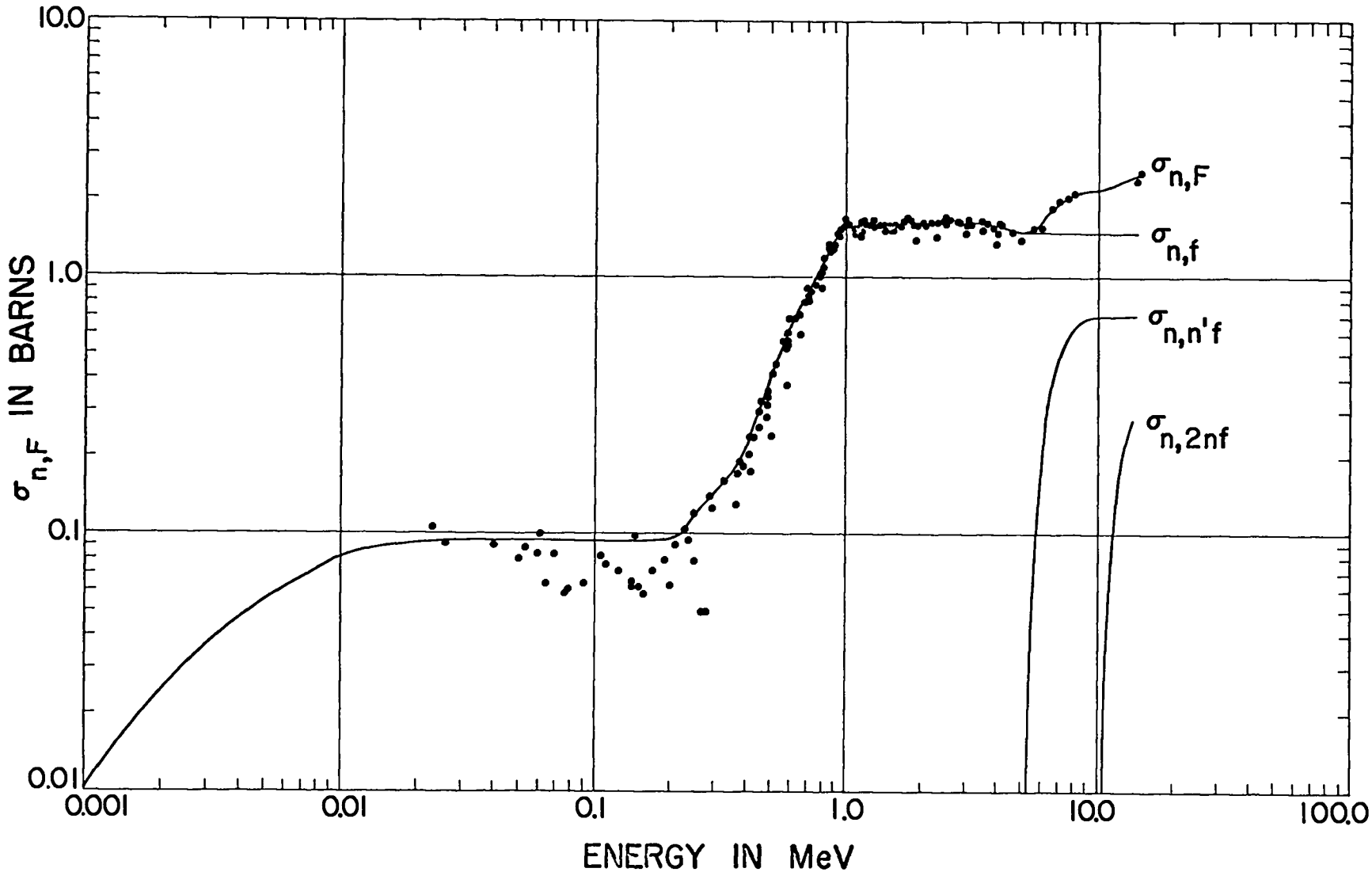

Fig. 13. Fission cross section for ^{240}Pu.

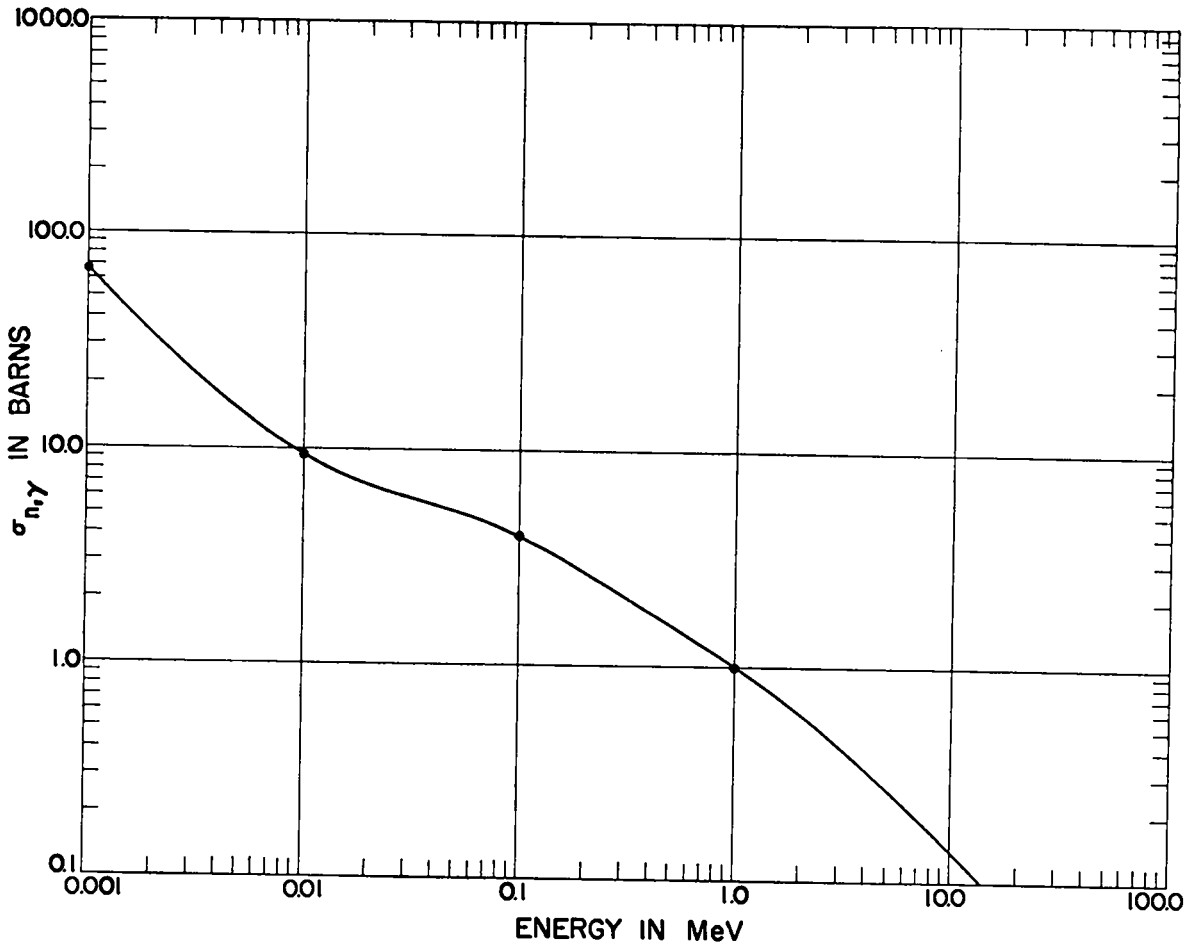

Fig. 14. Radiative capture cross section for ^{240}Pu.

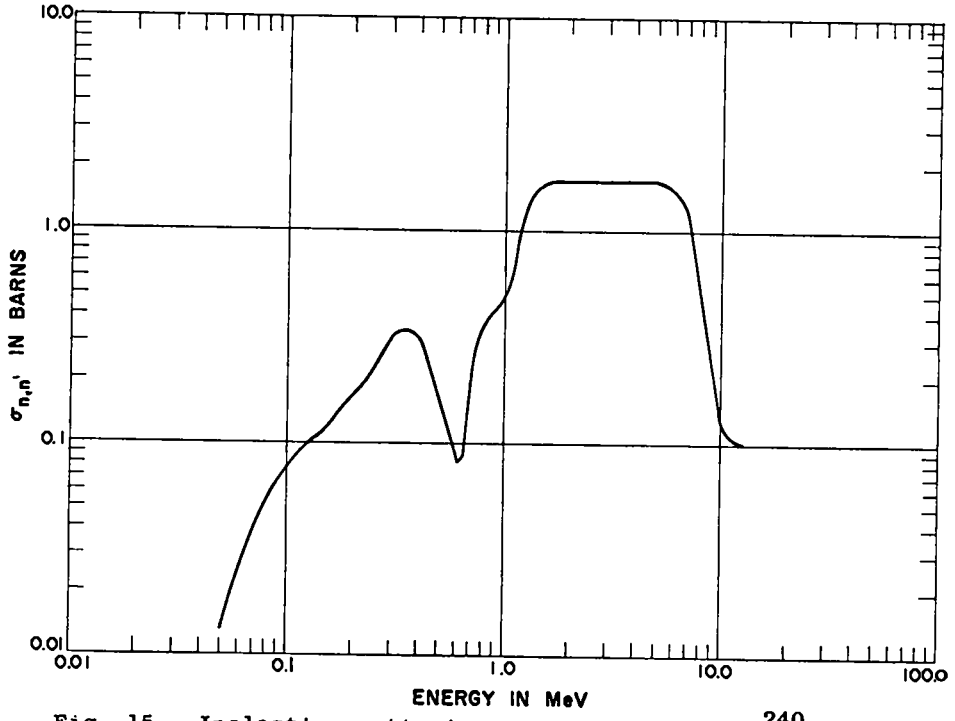

Fig. 15. Inelastic scattering cross section for ^{240}Pu.

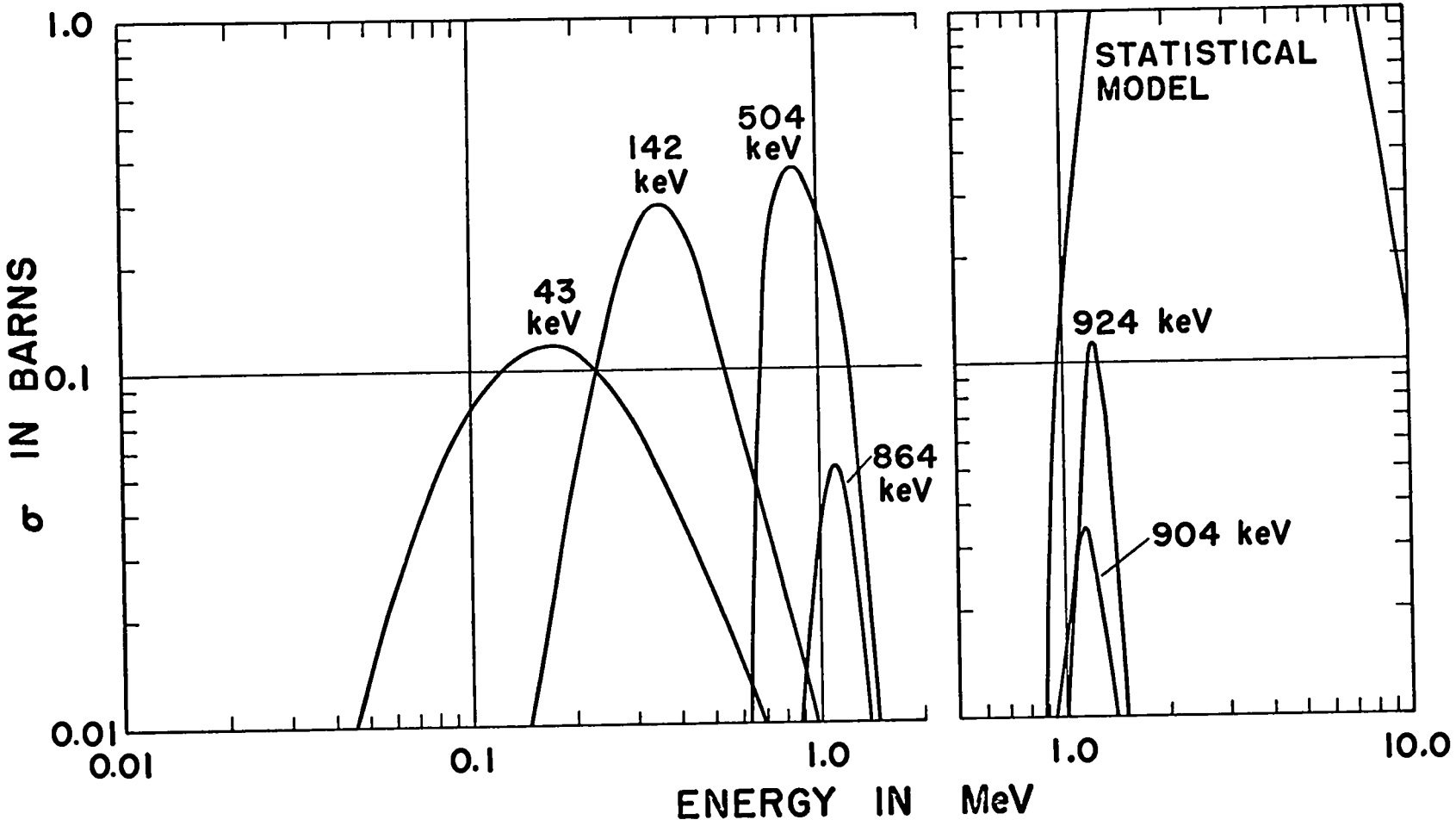

Fig. 16. Partial inelastic scattering cross sections for ^{240}Pu.

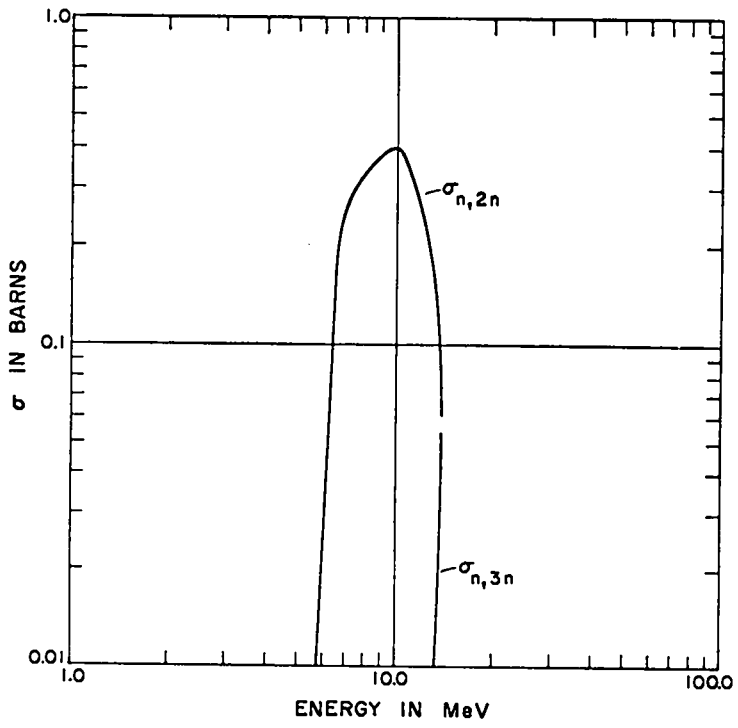

Fig. 17. $\sigma_{n,2n}$ and $\sigma_{n,3n}$ for ^{240}Pu.

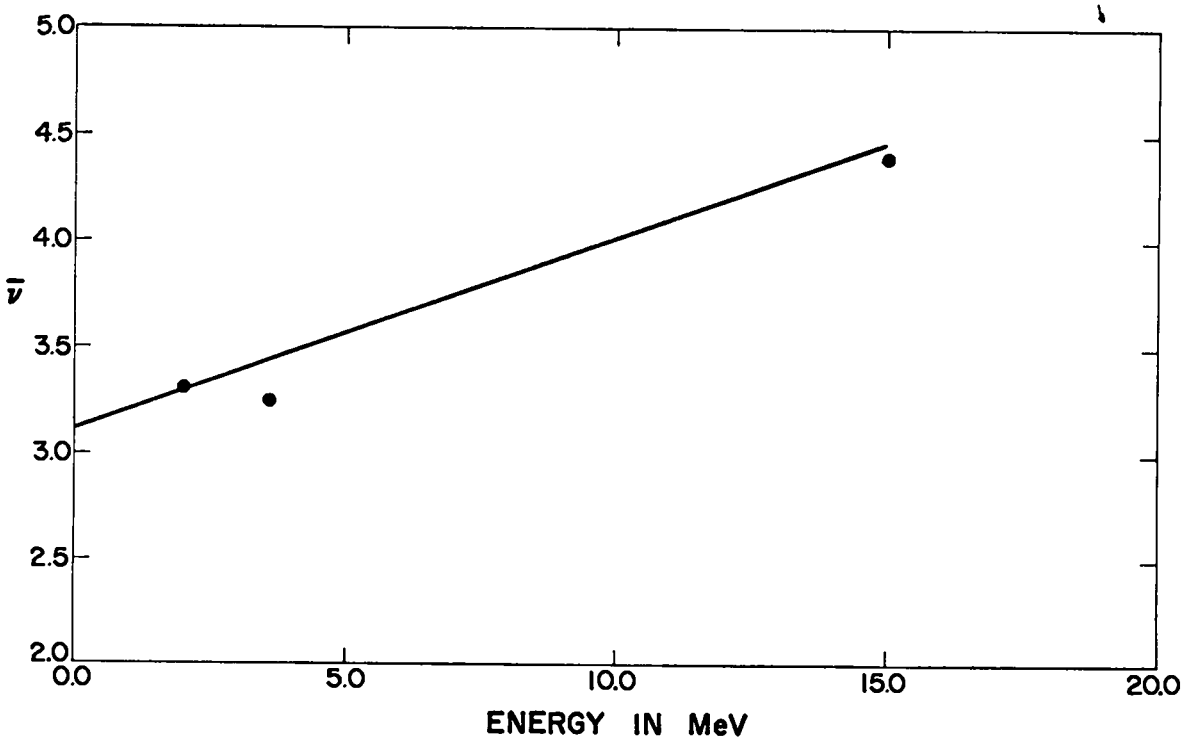

Fig. 18. Mean number of neutrons per fission for ^{240}Pu.